IEEE Photonics Journal
An IEEE Photonics Society Publication

Near-Infrared Femtosecond Laser for Studying the Strain in $Si_{1-x}Ge_x$ Alloy Films via Second-Harmonic Generation

Volume 2, Number 6, December 2010

Ji-Hong Zhao
Bu-Wen Cheng
Qi-Dai Chen
Wen Su
Ying Jiang
Zhan-Guo Chen
Gang Jia
Hong-Bo Sun, Member, IEEE

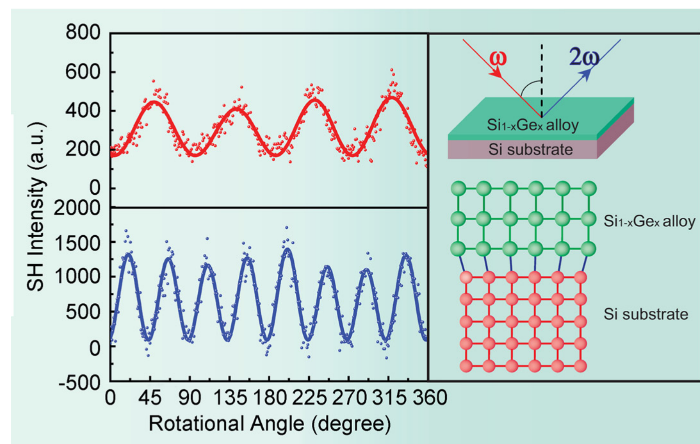

DOI: 10.1109/JPHOT.2010.2089976
1943-0655/$26.00 ©2010 IEEE

IEEE photonics SOCIETY

IEEE

Near-Infrared Femtosecond Laser for Studying the Strain in $Si_{1-x}Ge_x$ Alloy Films via Second-Harmonic Generation

Ji-Hong Zhao,[1] Bu-Wen Cheng,[2] Qi-Dai Chen,[1] Wen Su,[1] Ying Jiang,[1] Zhan-Guo Chen,[1] Gang Jia,[1] and Hong-Bo Sun,[1,3] *Member, IEEE*

[1]State Key Laboratory on Integrated Optoelectronics, College of Electronic Science and Engineering, Jilin University, Changchun 130023, China
[2]State Key Laboratory on Integrated Optoelectronics, Institute of Semiconductors, Chinese Academy of Sciences, Beijing 100083, China
[3]College of Physics, Jilin University, Changchun 130012, China

DOI: 10.1109/JPHOT.2010.2089976
1943-0655/$26.00 ©2010 IEEE

Manuscript received September 23, 2010; revised October 21, 2010; accepted October 21, 2010. Date of publication October 28, 2010; date of current version November 16, 2010. Corresponding authors: H.-B. Sun (e-mail: hbsun@jlu.edu.cn) and Q.-D. Chen (e-mail: chenqd@jlu.edu.cn).

Abstract: The second-harmonic generation (SHG) from $Si_{1-x}Ge_x$ alloy films has been investigated by near-infrared femtosecond laser. Recognized by *s*-out polarized SHG intensity versus rotational angle of sample, the crystal symmetry of the fully strained $Si_{0.83}Ge_{0.17}$ alloy is found changed from the O_h to the C_2 point group due to the inhomogeneity of the strain. Calibrated by double crystal X-ray diffraction, the strain-induced $\chi^{(2)}$ is estimated at 5.7×10^{-7} esu. According to the analysis on p-in/s-out SHG, the strain-relaxed $Si_{0.10}Ge_{0.90}$ alloy film is confirmed to be not fully relaxed, and the remaining strain is quantitatively determined to be around 0.1%.

Index Terms: Femtosecond laser, $Si_{1-x}Ge_x$ alloy, strain, second-harmonic generation, crystal symmetry.

1. Introduction

The near-infrared femtosecond laser has been widely used for fabricating 3-D microdevices [1], ultrafast spectroscopy, materials processing [2], and intense field physics. Also, the near-infrared femtosecond laser is an appropriate tool for studying strains of centrosymmetric semiconductor surface or interface via second-harmonic generation (SHG) [3]. Here, we apply the near-infrared femtosecond laser to investigate the crystal structure of $Si_{1-x}Ge_x$ alloys by SHG. We use the near-infrared femtosecond laser for two reasons. First, the near-infrared wavelength confines the detection range of the surface for semiconductors and therefore, the longitudinal resolution of SHG is improved. Second, the ultrashort laser pulse minimizes the thermal effect for retaining signal stability during SHG detection. SHG is a surface-and interface-sensitive optical probe method from which the structural information on the surface and interface of centrosymmetric semiconductors like silicon and germanium can be extracted. In our research, $Si_{1-x}Ge_x$ was chosen because it has drawn comprehensive attention as an attractive optoelectronic material. The cost of $Si_{1-x}Ge_x$ alloy is lower than that of III–V semiconductors, and it presents excellent compatibility with the present silicon technology [4]. Most importantly, the strained $Si_{1-x}Ge_x$ alloys would obviously enhance the carrier mobility more than the normal Si. That is because the electronic band structure of the crystal would be adjusted under uniaxial or biaxial strain. This leads to many practical applications.

There are mainly two current applications of $Si_{1-x}Ge_x$ alloy. The first usage is heterostructural devices based on biaxial-compressive strained $Si_{1-x}Ge_x$ films epitaxially grown on silicon [5], [6]. For example, the $Si_{1-x}Ge_x$ heterostructural bipolar transistors and the $Si_{1-x}Ge_x$ photodetectors at 1.3 or 1.55 μm have been widely applied to wireless communications [7], [8]. The second usage of the $Si_{1-x}Ge_x$ films is as a strain-relaxation virtual substrate for strained Si or quantum wells. This relaxed buffer substrate with obvious low dislocation density is highly important for the electrical and optical characteristics of Si devices. For instance, a strain-compensated quantum-well structure grown on strain-relaxed $Si_{1-x}Ge_x$ substrate can serve as a high-speed electro-absorption modulator [9]. So far, research on the structural symmetry of $Si_{1-x}Ge_x$ has mainly focused on superlattices, such as $(Ge_nSi_m)_p$ or Si/Ge_xSi_{1-x} periodic structures [10], [11]. Yet, the surface structure of $Si_{1-x}Ge_x$ alloy and the corresponding strain effect have rarely been investigated. To reach this end, our paper reports SHG as an effective approach for the quantitative determination of the $Si_{1-x}Ge_x$ film surface symmetry, as well as its strain-induced second-order nonlinear susceptibility.

2. Experiments

The $Si_{1-x}Ge_x$ alloy samples used in our experiments were prepared by ultra–high-vacuum chemical vapor deposition (UHV/CVD) with Si_2H_6 and GeH_4 gases as the reactive source. Two types of strain-state-$Si_{1-x}Ge_x$ alloy layers on Si (001) substrate were prepared. One of them is fully strained, while the other is strain relaxed. For the fully strained $Si_{0.83}Ge_{0.17}$ alloy film, a 200-nm-thick silicon buffer was directly grown on a Si (001) substrate, and then, the $Si_{0.83}Ge_{0.17}$ alloy film was deposited on it. Contrastively, for the strain-relaxed $Si_{0.10}Ge_{0.90}$ alloy, a low-temperature 10-nm-thick germanium layer was inserted between the alloy film and the Si substrate. The thicknesses of the strained $Si_{0.83}Ge_{0.17}$ and the strain-relaxed $Si_{0.10}Ge_{0.90}$ are 118 nm and 600 nm, respectively. The $Si_{0.83}Ge_{0.17}$ film thickness is less than the critical thickness; therefore, the film grew commensurately on Si with its plane lattice parameter matching the Si lattice parameter. For SHG measurements, a Ti: sapphire femtosecond laser from an oscillator with an 800-nm wavelength was used as the fundamental light. Using a femtosecond laser to study the SHG phenomenon can achieve high efficient SHG (peak intensity of femtosecond laser $\sim 10^{11}$ W/cm^2), minimize the surface/interface heating effect (low pulse energies $\sim$10 nJ) [12] further, and improve the longitudinal spatial resolution by its penetration depth ($\sim$100 nm for Si). The p-polarized beam obtained by rotating a half-wave plate was focused on the sample at 45° angle to generate SHG. The SHG signal was filtered by the $CuSO_4$ solution and an interference filter. Then, it was reflected into a photomultiplier tube with a lock-in amplifier. The s-polarized SH were selected by a polarization analyzer. A computer was employed to synchronously control a stepper motor to rotate the sample around the central axis.

3. Result and Discussions

In order to study the effect of strain on symmetry of $Si_{1-x}Ge_x$ alloys, the intensity of the s-polarized SHG under the s-polarized input were measured as a function of the rotational angle for the two samples. The experimental data is shown in Fig. 1. The s-polarized SHG output curves show eight-fold symmetry for the strain-relaxed $Si_{0.10}Ge_{0.90}$ alloy layer, which is similar to Si (001). In contrast, the strained $Si_{0.83}Ge_{0.17}$ alloy possesses four-fold symmetry in the SHG curves. The curves in Fig. 1 are then fitted by the following expression [11], [13]:

$$I_{s,s}^{(2\omega)}(\psi) \propto \left| \sum_{m=1}^{4} \left\{ a^{(m)}\cos[m(\psi+\psi_0)] + b^{(m)}\sin[m(\psi+\psi_0)] \right\} \right|^2 + h \tag{1}$$

where $I_{s,s}^{(2\omega)}(\psi)$ is the s-polarized SHG intensity, and the polarization state of the input fundamental light is s-polarized as well. The measurement started from an arbitrary angle ψ_0.

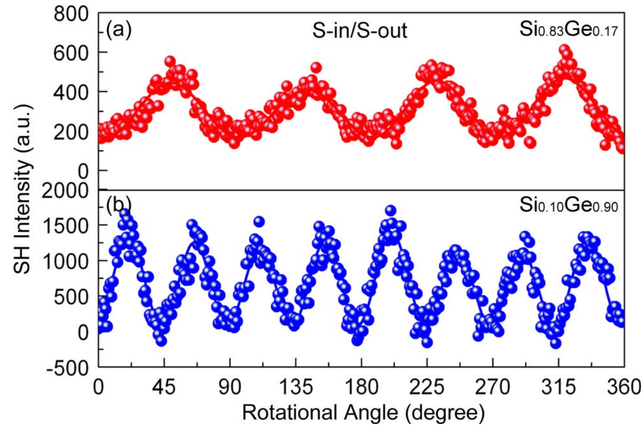

Fig. 1. S-in/s-out SH intensities as a function of rotational angle for (a) the fully strained $Si_{0.83}Ge_{0.17}$ alloy film and (b) strain-relaxed $Si_{0.10}Ge_{0.90}$ alloy film.

TABLE 1

Fourier coefficients fitted to the measured data of s-in/s-out SH intensity, which are normalized by the Fourier coefficient $C^{(4)}$ for each sample. We found the fitting result is not quite unique. For example, for $C^{(1)}$, we found that the value can range from 2.6 to 2.7 within a tolerance of 3.6%

Samples	$C^{(1)}$	$C^{(2)}$	$C^{(3)}$	$C^{(4)}$
$Si_{0.83}Ge_{0.17}$	2.7	84.9	4.0	1
$Si_{0.10}Ge_{0.90}$	0.02	0.05	0.01	1

Using Bottomley's processing method [13], the Fourier coefficients $C^{(m)}$ were obtained as

$$C^{(m)} = \bar{a}^{(m)^2} + \bar{b}^{(m)^2} \tag{2a}$$

$$\bar{a}^{(m)} = a^{(m)}\cos(m\psi_0) + b^{(m)}\sin(m\psi_0) = A^{(m)} + B^{(m)} \tag{2b}$$

$$\bar{b}^{(m)} = a^{(m)}\sin(m\psi_0) - b^{(m)}\cos(m\psi_0) = A^{(m)'} - B^{(m)'}. \tag{2c}$$

Using (1) as the fitting formula, the fitting curves are shown as solid lines in Fig. 1. After being normalized with $C^{(4)}$, the fitted Fourier coefficients of each item of the s-in/s-out polarization are shown in Table 1. The constant item h in (1) originates from the surface roughness, which is corresponding to the isotropic SHG contribution [14].

The different Fourier coefficients denote the origin of SHG: $C^{(1)}$ and $C^{(3)}$ are due to the miscut effect of the surface or the interface, which is displayed in the second-order nonlinear susceptibility $\chi^{(2)}$ [10], [15]. For our samples, the miscut angle is around 1°. $C^{(4)}$ coefficient originates from bulk quadrupole. Emphatically, $C^{(2)}$ represents the dipole-allowed effect; it includes surface-dipole-allowed and the bulk-dipole-allowed effects. The bulk-dipole effect possibly comes from the structural asymmetry of $Si_{1-x}Ge_x$ alloys. Another important contribution for the bulk-dipole effect is the strain-enhancement effect. Here, the strain enhancement mainly stems from the fact that the inhomogeneity of strain breaks the bulk centrosymmetry of the alloy. Therefore, a strain-induced second-order nonlinear susceptibility will contribute to the total SHG signal for our fully strained $Si_{0.83}Ge_{0.17}$ alloy [16], [17]. In addition, only around a 20-nm subsurface layer can be detected by SHG for the 800-nm fundamental light, and it is more indicative that the SHG is a sensitive optical detect method for the interface/surface. Fig. 2 shows the Fourier transform pattern of Fig. 1. Both the Fourier transform pattern and the Fourier coefficients (see Table 1) indicate the notable distinctions between the strained $Si_{0.83}Ge_{0.17}$ and the strain-relaxed $Si_{0.10}Ge_{0.90}$.

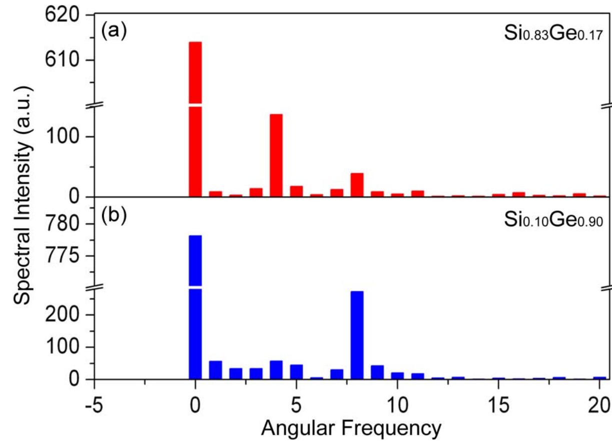

Fig. 2. Fourier transform of the azimuthal SH intensity patterns of Fig. 1 for (a) fully strained $Si_{0.83}Ge_{0.17}$ alloy film and (b) strain-relaxed $Si_{0.10}Ge_{0.90}$ alloy film.

Obviously, the four-fold frequency component is larger for $Si_{0.83}Ge_{0.17}$, and the eight-fold frequency component is larger for $Si_{0.10}Ge_{0.90}$ in the Fourier transform patterns. In fact, the largest difference between the strained and the strain-relaxed alloy layers is that the $C^{(2)}$ is the major contribution to the former, while the $C^{(4)}$ dominates the latter, as indicated in Table 1. The dominant $C^{(2)}$ for $Si_{0.83}Ge_{0.17}$ indicates that the large bulk-dipole contribution of $\chi^{(2)}$ was induced by strain; hence, the four-fold symmetry for this strain-induced $\chi^{(2)}$ is clearly observed in Fig. 1(a). It is generally accepted that strained $Si_{1-x}Ge_x$ alloys possess C_{4v} crystal symmetry. However, the strain-induced bulk-dipole contribution as the present study cannot exist for the C_{4v} symmetry in the s-in/s-out polarization combination according to phenomenological theory [18], but there is only bulk-quadrupole contribution, which means that the strained $Si_{0.83}Ge_{0.17}$ alloy here in fact holds C_2 symmetry instead of C_{4v} symmetry. This reduced symmetry could be possibly explained by the fact that the built-in strain effects for the different bonds of Si-Ge and Si-Si in the $Si_{0.83}Ge_{0.17}$ sample are not equivalent.

Next, we evaluate the contribution of strain effect to $\chi^{(2)}$. In fact, the stress in the $Si_{0.83}Ge_{0.17}$ alloy is biaxial due to lattice mismatch with Si substrate. Therefore, the built-in strain induces enhancement of SHG, and the nonlinear susceptibility $\chi^{(2)}$ follows the relation [19], [20]:

$$\left|\frac{\chi^{(2)}}{\chi^{(1)}}\right| = \left|\frac{3e}{2E_g}\frac{2(V_{strain}\times\zeta_0)\tau}{E_g}\right| \tag{3}$$

where the linear susceptibility $\chi^{(1)} = 0.916$ esu [21], and the bandgap $E_g = 1.03$ eV [22]. $\tau = (\sqrt{3}/4)a = 2.37$ Å denotes the nearest-neighbor separation of atoms [20], and $V_{strain} = 6.1$ eV is the deformation potential [23], which was calculated by the linear interpolation with the data in [23]. ζ_0 is the strength of the lattice deformation, which is decided by double crystal X-ray diffraction (DCXRD). The good crystal quality recognized by its quite narrow half peak width (159 arc sec) of the DCXRD curve in Fig. 3 was attained across the entire sample, showing the high uniformity of the $Si_{0.83}Ge_{0.17}$ alloy film. Its strain can be defined by the following expression:

$$\varepsilon = \frac{a^{\perp}_{Si_{1-x}Ge_x} - a_{Si_{1-x}Ge_x}}{a_{Si_{1-x}Ge_x}}. \tag{4}$$

Here, $a^{\perp}_{Si_{1-x}Ge_x}$ is the lattice constant of strained $Si_{1-x}Ge_x$ alloy along [001] growing direction and is determined by the DCXRD as 0.5494 nm for $Si_{0.83}Ge_{0.17}$. $a_{Si_{1-x}Ge_x}$ is the lattice constant of

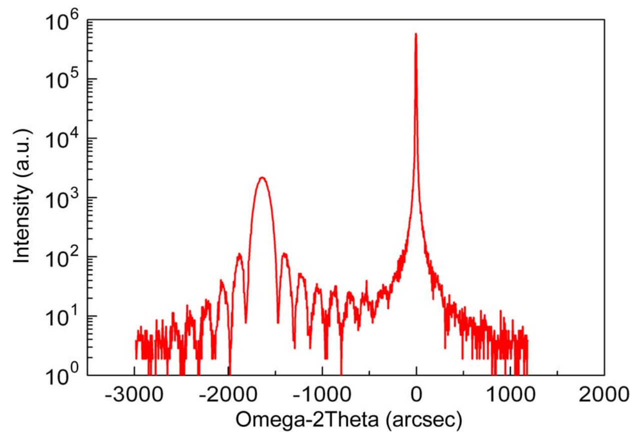

Fig. 3. Double crystal X-ray diffraction (DCXRD) of fully strained $Si_{0.83}Ge_{0.17}$ alloy film.

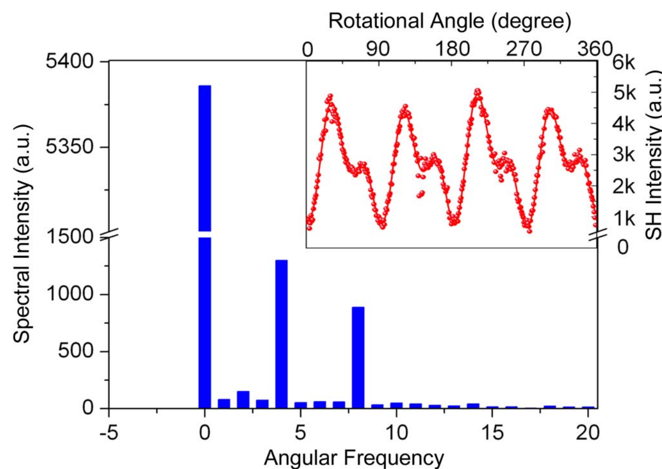

Fig. 4. P-in/s-out SH intensity versus azimuthal angles and its Fourier transform for $Si_{0.10}Ge_{0.90}$.

unstrained $Si_{1-x}Ge_x$ alloy. It can be calculated to 0.5466 nm for $x = 0.17$. Therefore, the strain is compressive with a magnitude of 0.51%. Therefore, the strain-induced second-order susceptibility $\chi^{(2)}$ can be calculated as 5.7×10^{-7} esu.

Similarly, the SHG signal of the p-in/s-out polarization for the $Si_{0.10}Ge_{0.90}$ sample is measured. The azimuthal-angle-dependent SHG and the corresponding Fourier transform pattern are shown in Fig. 4. The eight peaks and the fourfold symmetry indicate that the strain was not fully relaxed for the so-called strain-relaxed $Si_{0.10}Ge_{0.90}$ alloy. In order to ensure the case, the sample was further measured by DCXRD, and the experimental curve is shown in Fig. 5. As we see in the Fourier transform pattern, the remaining strain can be deduced to be approximately 0.1%. However, the remaining stress that exists in the strain-relaxed thin film could not change the symmetry of the epitaxial layer, and therefore, the $Si_{0.10}Ge_{0.90}$ alloy keeps the O_h symmetry. In order to make sure whether some other factors would affect our experimental results, the quality of the samples must be considered, and, especially, three points should be focused on homogeneity, surface roughness, and density of dislocations. First, from the AFM analysis, it is confirmed that the two alloy samples are relatively homogeneous. Second, still based on the AFM analysis, the surface roughness can be evaluated as 0.151 nm and 0.888 nm for fully strained $Si_{0.83}Ge_{0.17}$ and strain-relaxed $Si_{0.10}Ge_{0.90}$, respectively. Finally, the density of dislocations for the samples is as low as

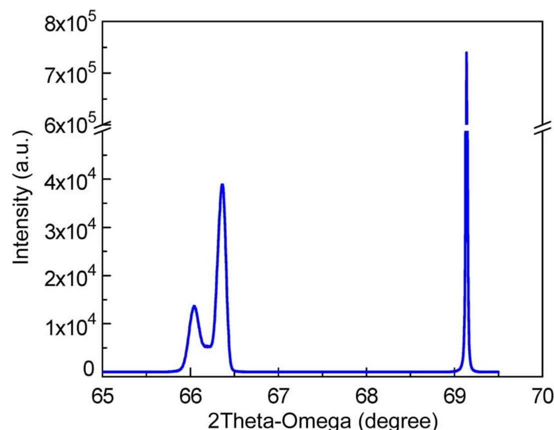

Fig. 5. Double crystal X-ray diffraction (DCXRD) of strain-relaxed $Si_{0.10}Ge_{0.90}$ alloy film.

about 10^6 cm^{-2}. Therefore, these effects can be neglected, and the present discussions should be reasonable.

4. Conclusion

In conclusion, the near-infrared femtosecond laser was used for studying of SHG from the strained and the strain-relaxed $Si_{1-x}Ge_x$ alloy films growing on the (001) silicon substrate. The dependence of s-in/s-out SHG on the azimuthal angle reveals that the point group symmetry of the strained $Si_{0.83}Ge_{0.17}$ alloy has been changed from O_h to C_2. The strain-induced part of SHG is dominant for the sample, and the corresponding second-order susceptibility $\chi^{(2)}$ is estimated to be 5.7×10^{-7} esu. Further studies also show that the strain-relaxed $Si_{0.10}Ge_{0.90}$ sample in fact has a minor remaining strain of 0.1% but that the crystal symmetry is retained. The present study exhibits that SHG is a sensitive and effective method of determining surface structure for the $Si_{1-x}Ge_x$ alloy or even other technically important semiconductors.

References

[1] S. Kawata, H. B. Sun, T. Tanaka, and K. Takada, “Final features for functional microdevices,” *Nature*, vol. 412, no. 6848, pp. 697–698, Aug. 2001.
[2] H. Wang, S. Lin, J. P. Allen, J. C. Williams, S. Blankert, C. Laser, and N. W. Woodbury, “Protein dynamics control the kinetics of initial electron transfer in photosynthesis,” *Science*, vol. 316, no. 5825, pp. 747–750, May 2007.
[3] W. Daum, H.-J. Krause, U. Reichel, and H. Ibach, “Identification of strained silicon layers at Si-SiO_2 interfaces and clean Si surfaces by nonlinear optical spectroscopy,” *Phys. Rev. Lett.*, vol. 71, no. 8, pp. 1234–1237, Aug. 1993.
[4] Y. Ishikawa and K. Wada, “Near-infrared Ge photodiodes for Si photonics: Operation frequency and an approach for the future,” *IEEE Photon. J.*, vol. 2, no. 3, pp. 306–320, Jun. 2010.
[5] D. J. Paul, “Si/SiGe heterostructures: From material and physics to devices and circuits,” *Semicond. Sci. Technol.*, vol. 19, no. 10, pp. R75–R108, Oct. 2004.
[6] Y. Shiraki and A. Sakai, “Fabrication technology of SiGe hetero-structures and their properties,” *Surf. Sci. Rep.*, vol. 59, no. 7/8, pp. 153–207, Nov. 2005.
[7] R. L. Jiang, Z. Y. Lo, W. M. Chen, L. Zang, S. M. Zhu, X. B. Liu, X. M. Cheng, Z. Z. Chen, P. Chen, P. Han, and Y. D. Zheng, “Normal-incidence SiGe/Si photodetectors with different buffer layers,” *J. Vac. Sci. Technol. B, Microelectron. Process. Phenom.*, vol. 18, no. 3, pp. 1251–1253, May 2000.
[8] J. S. Rieh, B. Jagannathan, D. R. Greenberg, M. Meghelli, A. Rylyakov, F. Guarin, Z. J. Yang, D. C. Ahlgren, G. Freeman, P. Cottrell, and D. Harame, “SiGe heterojunction bipolar transistors and circuits toward terahertz communication applications,” *IEEE Trans. Electron Devices*, vol. 52, no. 10, pp. 2390–2408, Oct. 2004.
[9] J. F. Liu, M. Beals, A. Pomerene, S. Bernardis, R. Sun, J. Cheng, L. C. Kimerling, and J. Michel, “Waveguide-integrated, ultralow-energy GeSi electro-absorption modulators,” *Nat. Photon.*, vol. 2, no. 7, pp. 433–437, Jul. 2008.
[10] G. Lüpke, D. J. Bottomley, and H. M. van Driel, “SiO_2/Si interfacial structure on vicinal Si(100) studied with second-harmonic generation,” *Phys. Rev. B, Condens. Matter*, vol. 47, no. 16, pp. 10 389–10 394, Apr. 1993.
[11] X. H. Zhang, Z. H. Chen, L. Z. Xuan, S. H. Pan, and G. Z. Yang, “Enhancement of bulklike second-order nonlinear susceptibility in SiGe/Si step wells and biasing-field controlled $(Si_5Ge_5)_{100}$ superlattices,” *Phys. Rev. B, Condens. Matter*, vol. 56, no. 24, pp. 15 842–15 846, Dec. 1997.

[12] J. I. Dadap, X. F. Hu, N. M. Russell, J. G. Ekerdt, J. K. Lowell, and M. C. Downer, "Analysis of second-harmonic generation by unamplified, high-repetition-rate ultrashort laser pulses at Si(001) interfaces," *IEEE J. Sel. Topics Quantum Electron.*, vol. 1, no. 4, pp. 1145–1155, Dec. 1995.
[13] D. J. Bottomley, G. Lüpke, J. G. Mihaychuk, and H. M. van Driel, "Determination of the crystallographic orientation of cubic media to high resolution using optical harmonic generation," *J. Appl. Phys.*, vol. 74, no. 10, pp. 6072–6078, Nov. 1993.
[14] O. A. Aktsipetrov, I. M. Baranova, and Y. A. Il'inskiĭ, "Surface contribution to the generation of reflected second-harmonic light for centrosymmetric semiconductors," *Sov. Phys.—JETP*, vol. 64, no. 1, pp. 167–173, Jul. 1986.
[15] G. Lüpke, D. J. Bottomley, and H. M. van Driel, "Second- and third-harmonic generation from cubic centrosymmetric crystals with vicinal faces: Phenomenological theory and experiment," *J. Opt. Soc. Amer. B, Opt. Phys.*, vol. 11, no. 1, pp. 33–44, Jan. 1994.
[16] J. Y. Huang, "Probing inhomogeneous lattice deformation at interface of $Si(111)/SiO_2$ by optical second-harmonic reflection and Raman spectroscopy," *Jpn. J. Appl. Phys.*, vol. 33, no. 7A, pp. 3878–3886, Jul. 1994.
[17] S. V. Govorkov, V. I. Emel'yanov, N. I. Koroteev, G. I. Petrov, I. L. Shumay, and V. V. Yakovlev, "Inhomogeneous deformation of silicon surface layers probed by second-harmonic generation in reflection," *J. Opt. Soc. Amer. B, Opt. Phys.*, vol. 6, no. 6, pp. 1117–1124, Jun. 1989.
[18] J. E. Sipe, D. J. Moss, and H. M. van Driel, "Phenomenological theory of optical second- and third-harmonic generation from cubic centrosymmetric crystals," *Phys. Rev. B, Condens. Matter*, vol. 35, no. 3, pp. 1129–1141, Jan. 1987.
[19] C. Zhang, X. D. Xiao, N. Wang, K. K. Fung, M. M. T. Loy, Z. H. Chen, and J. M. Zhou, "Defect-enhanced second-harmonic generation in $(Si_mGe_n)_p$ superlattices," *Appl. Phys. Lett.*, vol. 72, no. 17, pp. 2072–2074, Apr. 1998.
[20] J. C. Phillips and R. A. Van Vechten, "Nonlinear optical susceptibilities of covalent crystals," *Phys. Rev.*, vol. 183, no. 3, pp. 709–711, Jul. 1969.
[21] L. Friedman and R. A. Soref, "Second-order optical susceptibility of strained GeSi/Si superlattices," *J. Appl. Phys.*, vol. 61, no. 6, pp. 2342–2346, Mar. 1987.
[22] D. Dutartre, G. Brémond, A. Souifi, and T. Benyattou, "Excitonic photoluminescence from Si-capped strained $Si_{1-x}Ge_x$ layers," *Phys. Rev. B, Condens. Matter*, vol. 44, no. 20, pp. 11 525–11 527, Nov. 1991.
[23] T. P. Pearsall, *Strained-Layer Superlattices: Physics, Semiconductors and Semimetals*. New York: Academic, 1990, p. 27.